



REGULAR ARTICLE

A Compact Wideband Microstrip Patch Antenna Using a Partial Ground Plane for 28 GHz mmWave Applications

Md. Tanvir Rahman Jim^{1,*} , Intan Izafina Idrus², Naymaa Rashid³

¹ Department of EECE, Pabna University of Science and Technology, Pabna-6600, Bangladesh

² School of Engineering, Taylor's University, Taylor's Lakeside Campus, No. 1 Jalan Taylor's, 47500, Subang Jaya, Selangor DE, Malaysia

³ Department of Electrical and Electronic Engineering, Pabna University of Science and Technology, Pabna 6600, Bangladesh

(Received 02 February 2026; revised manuscript received 19 April 2026; published online 29 April 2026)

Millimeter-wave (mmWave) communication is a fundamental enabler for next-generation wireless systems due to its capability to support ultra-high data rates and massive network capacity. However, the design of compact antennas operating at mmWave frequencies remains challenging because conventional microstrip patch antennas suffer from inherently narrow impedance bandwidth and limited radiation efficiency. This paper presents a compact wideband microstrip patch antenna operating at the 28-GHz band using a slot-engineered radiating structure combined with a partial ground plane. The antenna is fabricated on a Rogers RT5880 substrate ($\epsilon_r = 2.2$, $\tan\delta = 0.0009$) with overall dimensions of $20 \times 21 \times 0.79$ mm³. Bandwidth enhancement is achieved by introducing multiple resonant perturbations through strategically positioned slots, which effectively alter surface current distribution and reduce the antenna quality factor. The proposed antenna achieves a -10 dB impedance bandwidth of 4.88 GHz (26.88-31.76 GHz), specifically covering n257 (26.5-29.5 GHz), n258 (24.25-27.5 GHz), and n261 (27.5-28.35 GHz) bands fully covering the targeted 28-GHz mmWave band. At the resonance frequency, the antenna demonstrates a return loss of -46.91 dB, VSWR of 1.009, peak gain of 6.45 dB, and radiation efficiency exceeding 92%. Electromagnetic analysis confirms that the slot configuration generates multiple coupled resonant modes, enabling broadband performance while preserving radiation stability. Comparative analysis with recently reported mmWave antennas demonstrates that the proposed design achieves a favorable trade-off between compact size, bandwidth, and radiation performance. These characteristics make the antenna a strong candidate for 5G, beyond-5G, and emerging 6G millimeter-wave communication systems.

Keywords: Microstrip patch antenna, Partial ground plane, CST, VSWR, 28 GHz mmWave applications, 5G.

DOI: [10.21272/jnep.18\(2\).02027](https://doi.org/10.21272/jnep.18(2).02027)

PACS number: 84.40.Ba

1. INTRODUCTION

The rapid growth of data-intensive wireless applications has significantly increased the demand for high-capacity communication systems. Consequently, millimeter-wave (mmWave) frequencies have emerged as a key enabler for modern wireless technologies, including satellite communications, 5G, Beyond-5G (B5G), and future 6G networks [1, 2]. In particular, the 28-38 GHz spectrum has attracted considerable research attention due to its wide bandwidth availability, high data-rate capability, and relatively low atmospheric absorption [3, 4]. To support ultra-fast connectivity and low latency, 5G networks operate across multiple spectrum layers ranging from sub-6 GHz to mmWave bands, where mmWave frequencies enable extremely high throughput and large channel capacity [5].

Among various antenna technologies, microstrip patch antennas (MPAs) remain widely adopted due to their low profile, compact structure, ease of fabrication, and compatibility with RF front-end circuitry [6, 7]. However, conventional MPAs suffer from limited impedance bandwidth and moderate gain. From an elec-

tromagnetic standpoint, this limitation arises from the high-quality factor associated with the resonant cavity behavior of patch structures, typically restricting the bandwidth to approximately 2-5%. To address this challenge, several performance-enhancement techniques have been investigated, including defected ground structures (DGS), slot-loaded patches, and substrate modification [8, 9].

In 5G systems, frequency allocations vary across different geographical regions, with mmWave bands around 24-30 GHz widely adopted to support high-capacity wireless links. The large bandwidth available in these bands enables hotspot deployments capable of delivering extremely high throughput. Recent advances in antenna engineering have further improved system performance through compact array architectures, multi-resonant geometries, and integration with WiFi-5/6 and 5G communication platforms. Additionally, the adoption of artificial intelligence and machine learning techniques has accelerated antenna optimization by enabling data-driven prediction of parameters such as gain and directivity in complex MIMO structures.

* Correspondence e-mail: tanvirjim017@gmail.com



Dual-band antenna solutions have therefore become an important research direction, enabling simultaneous operation across sub-6 GHz and mmWave bands to improve spectral efficiency and system flexibility in next-generation wireless communication systems. 5G, the fifth-generation mobile network, utilizes multiple frequency bands to provide fast, low-latency, and high-capacity wireless connectivity. These bands are categorized into low, mid, and high frequencies, each tailored to meet the specific requirements of different applications. These bands will allow the deployment of hotspots providing very high throughput thanks to the large bandwidth available for operators Table 1 shows the 5G frequency band of the required spectrum [16].

Table 1 – The 5G frequency band of the required spectrum

Geographical Area	5G Frequency Band
Europe	24.25 – 27.5 GHz
China	24.25 – 27.5 GHz and 37 – 43.5 GHz
Japan	27.5 – 28.28 GHz
Korea	26.5 – 29.5 GHz
USA	27.5 – 28.35 GHz and 37 – 40 GHz

In [11], F. Xiao et al. introduced a structure-shared dual-band antenna achieving a large frequency ratio while maintaining compactness. Similarly, C. Han et al. [12] proposed a dual-band mmWave antenna optimized for stable radiation and adequate gain at high frequencies. While these designs demonstrated effective multi-band operation, challenges related to bandwidth enhancement and inter-element isolation remain significant at mmWave frequencies. Slot-based techniques have emerged as a practical approach for bandwidth and impedance improvement. Works [13, 18, 20] demonstrated that slot perturbations – such as U-shaped and slotted geometries – can effectively modify current distribution and enhance impedance matching without significantly increasing antenna size. However, excessive slot incorporation may introduce fabrication complexity and radiation pattern distortion. To mitigate severe free-space path loss at mmWave bands, array-based architectures have been extensively investigated. For example, L. C. Paul et al. [14] proposed a hexagonal microstrip array to improve spatial efficiency and gain performance. Similarly, M. Y. Mohamed et al. [17] developed a 2×2 patch array at 28 GHz, demonstrating that optimized element spacing and feeding networks significantly influence beam shaping and radiation efficiency. Nevertheless, array enlargement often increases structural complexity and coupling effects. Multi-band mmWave arrays operating at 28/38 GHz have also been reported. M. I. Ahmed et al. [15] and H. M. Marzouk et al. [16] addressed dual-band MIMO configurations with emphasis on impedance bandwidth and isolation control. Although these works achieved acceptable gain and compact dimensions, maintaining stable performance across both bands while preserving high isolation remains a design challenge. Material innovation has additionally played a critical role in high-frequency antenna performance. K.

Cuneray and N. Akcam [19] demonstrated that liquid crystal polymer (LCP) substrates can reduce dielectric loss while enabling flexible integration. Such materials are promising for compact mmWave terminals, though cost and fabrication constraints must be considered. Despite these contributions, existing designs still face trade-offs among compactness, bandwidth, gain enhancement, and inter-element isolation – particularly in dual-band mmWave MIMO configurations. Therefore, a structurally optimized antenna capable of maintaining stable radiation characteristics, enhanced impedance bandwidth, and improved isolation within compact dimensions remains highly desirable for next-generation 5G systems.

The major contributions of this work are summarized as follows:

1. A compact mmWave antenna structure suitable for integration in next-generation wireless systems.
2. A multi-slot perturbation technique that effectively broadens impedance bandwidth.
3. Electromagnetic analysis of current distribution and resonance coupling mechanisms.
4. Comparative performance evaluation with recently reported 28-GHz antennas.

The remainder of this paper is organized as follows: Section 2 describes the proposed antenna structure. Section 3 presents the simulated results and performance analysis. Finally, Section 4 concludes the paper and discusses key findings.

2. DESIGN STRUCTURE

The proposed compact wideband microstrip patch antenna operating at 28 GHz for millimeter-wave (mmWave) applications was designed, simulated, and optimized using CST Microwave Studio. The antenna is fabricated on a Rogers RT/duroid 5880 substrate characterized by a relative permittivity (ϵ_r) of 2.2, loss tangent of 0.0009, and thickness of 0.79 mm, providing low dielectric loss and stable electromagnetic performance at mmWave frequencies. The overall substrate size is 20×21 mm², while copper layers of 0.035 mm thickness are used for both the radiating patch and ground plane. The design process began with a conventional rectangular microstrip patch antenna employing a full ground plane, where the patch dimensions (11×18.2 mm²) were calculated to support the fundamental TM₁₀ resonance near 28 GHz. A microstrip feed line (11.5×2.4 mm²) was used to achieve 50 Ω impedance matching, and the ground plane size was initially set to 20×21 mm². However, this baseline configuration exhibited limited impedance bandwidth due to the high quality factor associated with the resonant cavity behavior of the conventional patch. To overcome this limitation, a slot-loading technique was implemented to enhance bandwidth and impedance matching. Two vertically symmetric rectangular slots (2.8×1.8 mm²) were introduced near the feed region to improve coupling and generate additional resonant modes, while a central square slot was added to perturb the dominant current distribution and reduce reactive energy concentration. Additional horizontal and corner rectangular slots were incorporated to fine-tune the impedance characteristics and broaden the operational bandwidth. The slot di-

mensions were optimized through parametric analysis to achieve constructive resonance coupling while preserving stable radiation behavior. Finally, the full ground plane was modified to a partial ground configuration ($20 \times 18 \text{ mm}^2$), which increased fringing fields and enhanced radiation from the feed region, further improving impedance bandwidth and matching. Through iterative optimization of slot parameters and ground plane length, the final wideband antenna configuration was achieved, with the optimized design parameters summarized in Table 2 and the three-dimensional structure illustrated in Fig. 1(c).

Table 2 – List of parameters

Symbol	Value (mm)
L	20
W	21
a	6
b	6.20
c	6
d	8.80
e	2
f	17
g	3
L_f	11.5
W_f	2.40
W_g	18

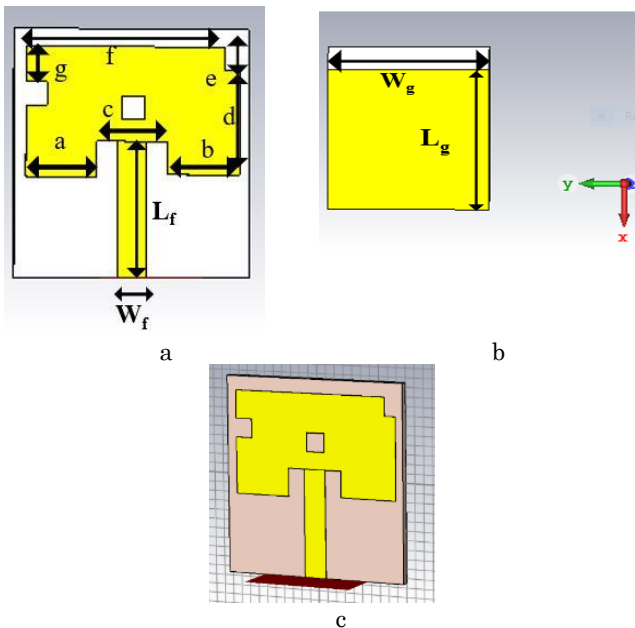


Fig. 1 – Proposed compact wideband Microstrip patch antenna: a – front view; b – back view; c – 3D view

3. RESULT AND DISCUSSION

Here, we have discussed about the results and analysis of the presented work. An antenna's return loss, or S11, indicates how much of the power that is delivered to the system is reflected back to its input point. Figure 2 displays the compact wideband microstrip patch antenna's simulated reflection coefficient. The evaluated resonant mode is the center frequency of the antenna, which is 28 GHz. It demon-

strates that the resonance frequency of 28 GHz and the -46.91 dB S11 value of the proposed antenna have been achieved. The frequency range at which an antenna can effectively transmit or receive radiation is known as its bandwidth. The frequency range of operation for this antenna is 26.88 to 31.76 GHz.

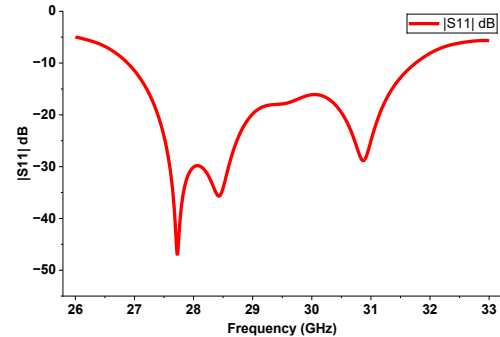


Fig. 2 – Reflection coefficient of the proposed antenna

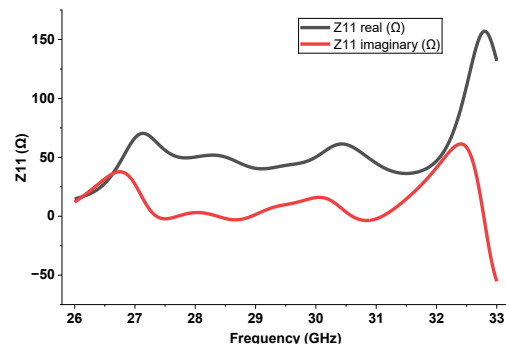


Fig. 3 – Z-parameters of the proposed antenna

Since Z parameters are essentially the voltage-to-current ratios, they are also known as impedance parameters. The Z parameter has both real and imaginary parts. An effective antenna has a real part of about fifty and an imagined part of almost zero. The Z parameter of the proposed compact wideband microstrip patch antenna is shown in Figure 3. The antenna's center frequency is 28 GHz, and its Z parameter has a real part of 50.12Ω and an imaginary part that is close to zero.

s

Fig. 4 – VSWR of the proposed antenna

Better impedance matching and more efficient power transfer via radio or wireless transmission to the antenna are indicated by a low VSWR rating. The VSWR spectrum fluctuations of the 28 GHz antenna are shown in Figure 4. The provided antenna's excellent VSWR of 1.009 at the center frequency of 28 GHz is shown in the figure. One of the main design requirements for the suggested antenna was a VSWR of less than 1.5 at center frequency, which this value fulfills. At the lower cutoff frequency of 26.88 GHz, the VSWR is 1.92. However, the VSWR is 1.92 at the highest cutoff point, which is at 31.76 GHz. This shows how the 27.73 GHz small wideband microstrip patch antenna has a VSWR of less than 2 and can cover the 26.88 to 31.76 GHz range.

When an antenna has a high radiation efficiency (efficiency factor), its directivity is greater than its gain. The corresponding area of Figure 5 displays the directivity, linear gain, and working frequency range. With a central frequency of 28 GHz, the proposed antenna in this study has a higher directivity (5.80 dBi) and acquired gain (5.34 dB), which makes it a desirable option for use in 28 GHz mmWave applications. The directivity and gain values range from 4.83 to 6.84 dBi and 4.48 to 6.45 dB, respectively, for an operating frequency of 26.88 to 31.76 GHz. At 28.45 GHz, this miniature wideband antenna offers a peak gain of 6.45 dB and a peak directivity of 6.84 dBi. The 3D directivity and gain at the center frequency of 28GHz are shown in Figures 6 and 7, respectively. These 3D evaluations also show an antenna with 5.34 dB gain and 5.80 dBi directivity at 28 GHz.

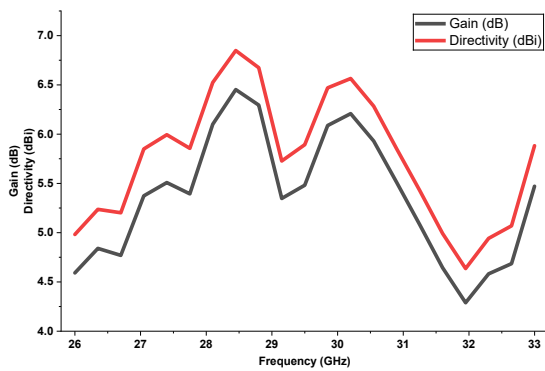


Fig. 5 – Linear gain and directivity of the proposed antenna

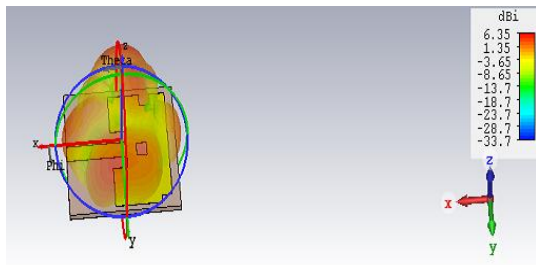


Fig. 6 – Directivity at 28 GHz of the proposed antenna

Antenna economic effectiveness can be calculated with the help of antenna efficiency. The estimated radiation efficiency of the compact, wideband antenna based on a partial ground plane is shown in Figure 8. At the center frequency is 28 GHz, the observed simulation efficiency is 89.95 %. At the lower cut off limit of 26.88 GHz, the efficiency is 90.05 %. At the highest cut off frequency of 31.76 GHz, the efficiency is 92.31 %.

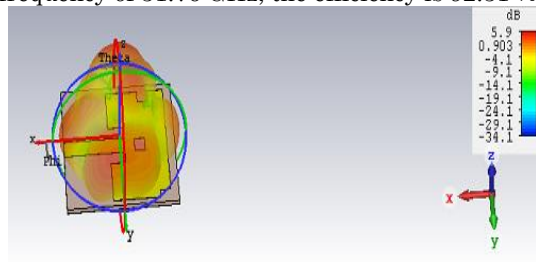


Fig. 7 – Gain at 28 GHz of the proposed antenna

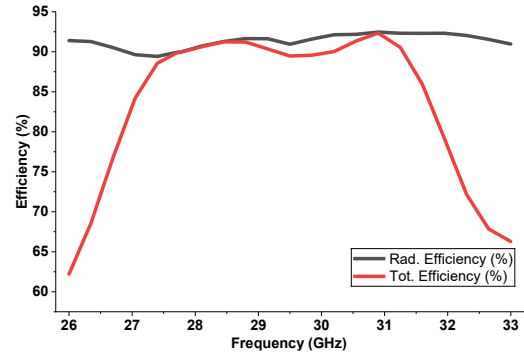


Fig. 8 – Efficiency of the proposed antenna

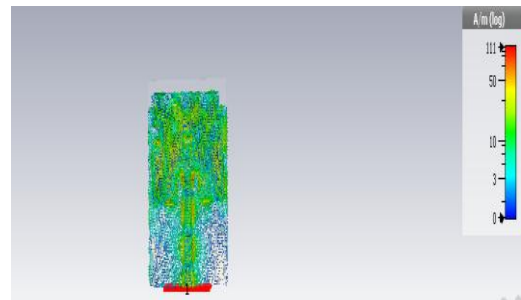
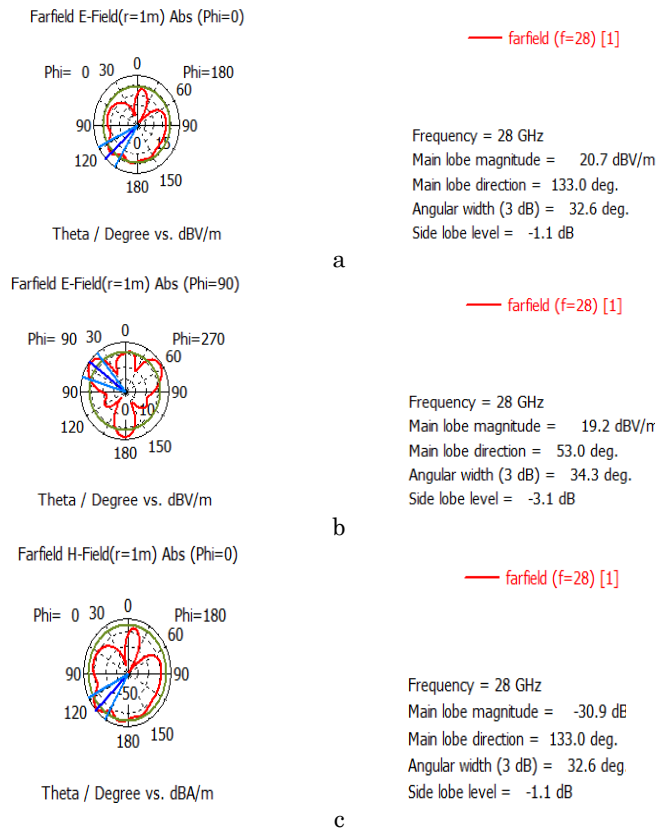


Fig. 9 – Surface current of the proposed antenna

The greatest efficiency of this wideband antenna, which uses partial ground plane technology, is 92.46 % at 30.9 GHz. Figure 9 illustrates the surface current distribution on the proposed antenna at 28 GHz. The current density peaks at the patch edges, reaching 110.91 A/m



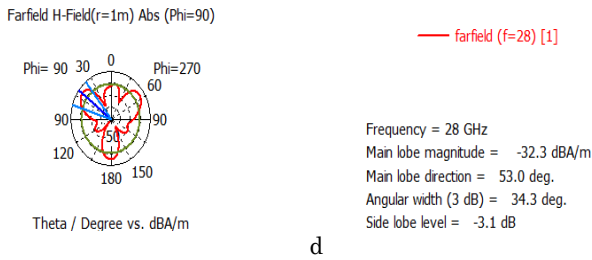


Fig. 10 – *E* and *H* fields of the proposed antenna: a – *E*-Field at $\phi = 0^\circ$; b – *E*-Field at $\phi = 90^\circ$; c – *H*-Field at $\phi = 0^\circ$; d – *H*-Field at $\phi = 90^\circ$

Figure 10 shows several polar plots of radiation patterns from the low profile 5G antenna at 28 GHz (a, b, c, and d). The *E* field patterns are displayed in Fig. 10 (a and b), while the *H* field patterns are shown in Figure 10 (c, d). The polar plot of the radiation pattern shows that the primary lobe is pointed at 133 for $\phi = 0^\circ$ and 53° for $\phi = 90^\circ$. The half power beamwidth (HPBW), also known as 3 dB angular beam width, is 32.6° for $\phi = 0^\circ$ and 34.3° for $\phi = 90^\circ$. The *E*-field's main lobe magnitude ranges from 20.7 dBV/m at $\phi = 0$ to 19.3 dBV/m at $\phi = 90^\circ$. Similarly, for the *H*-field, the major lobe magnitude is -30.9 dBA/m at $\phi = 0^\circ$ and -32.3 dBA/m at $\phi = 90^\circ$. It is worth sharing that the lowest side lobe level (LSLL) is -1.8 dB at $\phi = 90^\circ$. Table III compares the designed antenna with recently published 5G antennas. The proposed design achieves a wider bandwidth in the 28 GHz 5G band, along with good gain and a compact size.

Table 3 – Compare the designed antenna with recently published 5G antennas

Reference No	Resonant frequency (GHz)	Return loss (dB)	Bandwidth (GHz)	Maximum Gain(dB)	Size (W×L) (mm ²)	Substrate material
[11]	28	≈ -30	1.5	9.9	33×44	TLY-5 0200
[12]	≈ 27.4	-30	9.1	2.3	4×9.45	Material ($\epsilon_r = 4.4$)

REFERENCES

- L.C. Paul et al., *International Conference on Science & Contemporary Technologies (ICSCT)* (2021) <https://doi.org/10.1109/ICSCT53883.2021.9642597>.
- L.C. Paul et al., *International Conference on Science & Contemporary Technologies (ICSCT)* (2021) <https://doi.org/10.1109/ICSCT53883.2021.9642644>.
- L.C. Paul et al., *2021 IEEE Joint 10th International Conference on Informatics, Electronics & Vision (ICIEV) and 2021 5th International Conference on Imaging, Vision & Pattern Recognition (icIVPR)* (2021) <https://doi.org/10.1109/ICIEVicIVPR52578.2021.9564160>.
- L.C. Paul et al., *International Conference on Electronics, Communications and Information Technology (ICECIT)* (2021). <https://doi.org/10.1109/ICECIT54077.2021.9641479>.
- L.C. Paul et al., *International Conference on Electronics, Communications and Information Technology (ICECIT)* (2021) <https://doi.org/10.1109/ICECIT54077.2021.9641442>


[13]	38	≈ -43	22	4	5×5	Rogers RT 5880
[14]	28.49	-39.55	0.814	8.841	35×36	Teflon
[15]	≈ 27.9	-	2.305	7.182	55 × 115	Rogers RT 5880
[16]	≈ 27.5	≈ -37	1.0683	7.88	55 × 110	Rogers RT 5880
[17]	≈ 28.5	≈ -75	4	23.8	44.10 × 42.6	Foam
[18]	≈ 27, 28.5, 31	≈ -20, -43, -31	4.14	14.3	41.3 × 46	Rogers RT 5880
[19]	28	-23.867	1.17	9.5	20 × 36	Rogers Ultralam 3850HT
[20]	28	-39.37	2.478	6.37	7 × 7	FR4
Proposed work	28	-46.91	4.88	6.45	21 × 20	Rogers RT 5880

4. CONCLUSION

This work demonstrates the design and validation of a compact wideband microstrip patch antenna tailored for 28 GHz mmWave systems. Fabricated on a Rogers RT 5880 substrate with overall dimensions of $20 \times 21 \times 0.79$ m³, the antenna employs a single rectangular radiating patch integrated with strategically engineered slots and a partial ground plane to enhance impedance matching and bandwidth. The proposed configuration achieves an excellent reflection coefficient of -46.91 dB at 28 GHz and provides a wide -10 dB impedance bandwidth of 4.88 GHz, covering 26.88-31.76 GHz. In addition, the antenna delivers a maximum gain of 6.45 dBi and a directivity of 6.85 dBi, ensuring stable radiation characteristics suitable for high-frequency applications. The combination of compact size, wide bandwidth, and satisfactory gain confirms the effectiveness of the design strategy and highlights its strong potential for integration into next-generation 28 GHz mmWave wireless communication systems. The proposed antenna provides an effective solution for 5G, beyond-5G, and future 6G wireless communication systems

- gation and USNC URSI Radio Science Meeting (2019).
13. J.L. Li, M.H. Luo, H. Liu, *Proceedings of the Progress In Electromagnetics Research Symposium*, 739 (2017).
 14. L.C. Paul, M.M. Alam, *Proceedings of the 3rd International Conference on Electrical Information and Communication Technology* (2017).
 15. M.I. Ahmed, H.M. Marzouk, A. Shaalan, *Proceedings of the 6th International Conference on Advanced Control Circuits and Systems & 5th International Conference on New Paradigms in Electronics & Information Technology*, 71 (2019).
 16. H.M. Marzouk, M.I. Ahmed, A.A. Shaalan, *Proceedings of the International Symposium on Antennas and Propagation and USNC-URSI Radio Science Meeting*, 607 (2019).
 17. M.Y. Mohamed, AM. Dini, M. M. Soliman, A.Z.M. Imran, *IEEE International Conference on Informatics, IoT, and Enabling Technologies*, 445 (2020).
 18. N. Yoon, C. Seo, *J. Electromagn. Eng. Sci.* 17 No 3, 133 (2017).
 19. K. Cuneray, N. Akcam, *3rd International Symposium on Multidisciplinary Studies and Innovative Technologies* (2019).
 20. A.F. Kaeib, N.M. Shebani, A.R. Zarek, *Proceedings of the 19th Int'l Conf. on Sciences and Techniques of Automatic Control and Computer Engineering*, 648 (2019).

Компактна широкосмугова мікросмужкова патч-антена з використанням часткової заземлювальної площини для застосувань міліметрового діапазону 28 ГГц

Md. Tanvir Rahman Jim¹ , Intan Izafina Idrus², Naymaa Rashid³

¹ Department of EECE, Pabna University of Science and Technology, Pabna-6600, Bangladesh

² School of Engineering, Taylor's University, Taylor's Lakeside Campus, No. 1 Jalan Taylor's, 47500, Subang Jaya, Selangor DE, Malaysia

³ Department of Electrical and Electronic Engineering, Pabna University of Science and Technology, Pabna 6600, Bangladesh

Міліметрово-хвильовий (mmWave) зв'язок є фундаментальним фактором для бездротових систем наступного покоління завдяки своїй здатності підтримувати надвисокі швидкості передачі даних та величезну ємність мережі. Однак, проектування компактних антен, що працюють на міліметрових хвилях, залишається складним завданням, оскільки звичайні мікросмужкові патч-антени мають вузьку смугу пропускання імпедансу та обмежену ефективність випромінювання. У цій статті представлено компактну широкосмугову мікросмужкову патч-антену, що працює в діапазоні 28 ГГц, з використанням випромінювальної структури з щілинами в поєднанні з частковою заземлювальною площиною. Антена виготовлена на підкладці Rogers RT5880 ($\epsilon_r \leq 2,2$, $\tan\delta \leq 0,0009$) із загальними розмірами $20 \times 21 \times 0,79$ мм³. Розширення смуги пропускання досягається шляхом введення кількох резонансних збурень через стратегічно розташовані щілини, які ефективно змінюють розподіл поверхневого струму та знижують добротність антени. Запропонована антена досягає смуги пропускання з імпедансом – 10 дБ 4,88 ГГц (26,88-31,76 ГГц), зокрема, охоплюючи діапазони n257 (26,5-29,5 ГГц), n258 (24,25-27,5 ГГц) та n261 (27,5-28,35 ГГц), повністю покриваючи цільовий ммхвильовий діапазон 28 ГГц. На резонансній частоті антена демонструє втрати на відбиття – 46,91 дБ, КСХН 1,009, пікове посилення 6,45 дБ та ефективність випромінювання понад 92 %. Електромагнітний аналіз підтверджує, що щілинна конфігурація генерує кілька зв'язаних резонансних мод, що забезпечує широкосмугову роботу, зберігаючи при цьому стабільність випромінювання. Порівняльний аналіз з нещодавно опублікованими ммхвильовими антенами показує, що запропонована конструкція досягає сприятливого компромісу між компактними розмірами, смугою пропускання та характеристиками випромінювання. Ці характеристики роблять антену сильним кандидатом для систем міліметрового зв'язку 5G, систем після 5G та нових 6G.

Ключові слова: Мікросмужкова патч-антена, Часткова площина заземлення, CST, VSWR, Застосування мм-хвиль 28 ГГц, 5G.